Kinetic Study of the Reaction of Ir($a^4F_{9/2}$) with CH_4, O_2, and N_2O

Mark L. Campbell†

Chemistry Department, United States Naval Academy, Annapolis, Maryland 21402

Received: July 14, 1997; In Final Form: September 30, 1997⊗

The gas-phase reactivity of ground-state Ir($a^4F_{9/2}$) with CH_4, O_2, and N_2O is reported. Iridium atoms were produced by the photodissociation of [$Ir(CO)_2$(acac)] and detected by laser-induced fluorescence. The reaction rate of the $a^4F_{9/2}$ state with CH_4 is very slow and temperature-dependent. The methane reaction is pressure-independent indicating a bimolecular reaction. The bimolecular rate constant from 398 to 498 K is described in Arrhenius form by $(7 \pm 5) \times 10^{-11}$ exp(-37 ± 3 kJ/mol/*RT*) where the uncertainties represent $\pm 2\sigma$. The reaction rates of the $a^4F_{9/2}$ state with O_2 and N_2O are pressure-dependent, indicating adduct formation. The limiting low-pressure third-order, k_0, and limiting high-pressure second-order, k_∞, room-temperature rate constants with O_2 in nitrogen buffer are $(4.8 \pm 1.6) \times 10^{-30}$ cm^6 s^{-1} and $(3.6 \pm 0.4) \times 10^{-12}$ cm^3 s^{-1}, respectively. For N_2O, k_0 and k_∞ are $(2.2 \pm 0.5) \times 10^{-33}$ cm^6 s^{-1} and $(5.9 \pm 0.8) \times 10^{-15}$ cm^3 s^{-1}, respectively. A lower limit for the activation energy for the abstraction of an oxygen atom from N_2O to produce IrO is estimated at 45 kJ/mol.

Introduction

Gas-phase transition-metal (TM) chemistry is an intriguing field of study due to the high multiplicities of the atomic ground states and the large number of low-lying metastable states. The early gas-phase work of TMs focused on the reactions of the cations due to the ability of mass spectrometric methods to selectively control the kinetic energy and electronic state of the reactant ion and to sensitively detect the products. An understanding of how the low-lying M^+ electronic states govern chemical reactivity is now fairly well established.[1−5]

Only recently have the reactions of the gas-phase neutral TM atoms received considerable attention. The most complete studies have been performed on the reactions with small alkenes and alkanes.[6−19] The majority of atoms in the 3d, 4d, and 5d series have now been studied and indicate the ground and low-lying states of the TM dramatically influence the reaction kinetics.[12]

The kinetics of the reactions of TM atoms with oxygen-containing oxidants has recently been an active field of study.[20−29] The cumulative data reported thus far indicate the electronic state is a very important factor in the dynamics of these reactions. For example, for both the abstraction and termolecular association channels with O_2, TMs with s^1d^{n-1} configurations have been found to be more reactive than their s^2d^{n-2} counterparts.[23−27]

In this paper we report a kinetic study of the $6s^25d^7$ $a^4F_{9/2}$ state of iridium with methane, oxygen, and nitrous oxide. The reporting of these reactions for iridium will further update the database of TM reactions and allow comparison of iridium's kinetic behavior with other TMs. Two surprising results will be reported for iridium. In contrast to the 3d metals with s^2d^{n-2} configurations, iridium is unusually reactive with O_2 in the termolecular association reaction. Iridium is also the first reported TM to react with N_2O through a termolecular mechanism. This study also reports on the temperature dependence of the reaction of iridium with methane which will allow for a comparison of the experimentally determined activation energy with theoretically calculated barriers reported previously.[11]

Experimental Section

Pseudo-first-order kinetic experiments ([Ir] ≪ [oxidant]) were carried out in an apparatus with slowly flowing gas using a laser photolysis/laser-induced fluorescence (LIF) technique. The experimental apparatus and technique have been described in detail elsewhere.[20] Briefly, the reaction chamber is a stainless steel reducing four-way cross with attached sidearms and a sapphire window for optical viewing. The reaction chamber is enclosed within a convection oven (Blue M, Model 206F) for temperature dependence experiments.

Iridium atoms were produced by the 248 nm photodissociation of dicarbonyl(acetylacetenato)iridium(I) [$Ir(CO)_2$(acac)] using the output of an excimer laser (Lambda Physics Lextra 200). Iridium atoms were detected via LIF using an excimer-pumped dye laser (Lambda Physics Lextra 50/ScanMate 2E) with a KDP doubling crystal tuned to the $z^6G_{11/2}^\circ \leftarrow a^4F_{9/2}$ transition at 292.479 nm.[30] The reported lifetime of the $z^6G_{11/2}^\circ$ state is 69 ns.[31] LIF signals from this state were strong even at high total pressures, indicating collisional quenching of this state was not a problem. The dye laser beam (diameter ∼ 4 mm) was centered within the cross-sectional area swept by the counter-propagated photolysis beam (diameter ∼ 12.5 mm), and the fluorescence was detected at 90° to the laser beams with a three-lens telescope imaged through an iris. A photomultiplier tube (Hamamatsu R375) was used in collecting the LIF which was subsequently sent to a gated boxcar sampling module (Stanford Research Systems SR250), and the digitized output was stored and analyzed by a computer.

The iridium precursor was entrained in a flow of nitrogen buffer gas. The precursor carrier gas, buffer gas, and reactant gases flowed through calibrated mass flow meters and flow controllers prior to admission to the reaction chamber. Each sidearm window was purged with a slow flow of buffer gas to prevent deposition of iridium and other photoproducts. Total flows were between 500 and 3800 sccm. Pressures were measured with MKS Baratron manometers, and chamber temperatures were measured with a thermocouple. The delay time between the photolysis pulse and the dye-laser pulse was varied by a digital delay generator (Stanford Research Systems DG535) controlled by a computer. The trigger source for these experiments was scattered pump laser light incident upon a fast

† Henry Dreyfus Teacher−Scholar.

⊗ Abstract published in *Advance ACS Abstracts,* November 1, 1997.

S1089-5639(97)02272-X

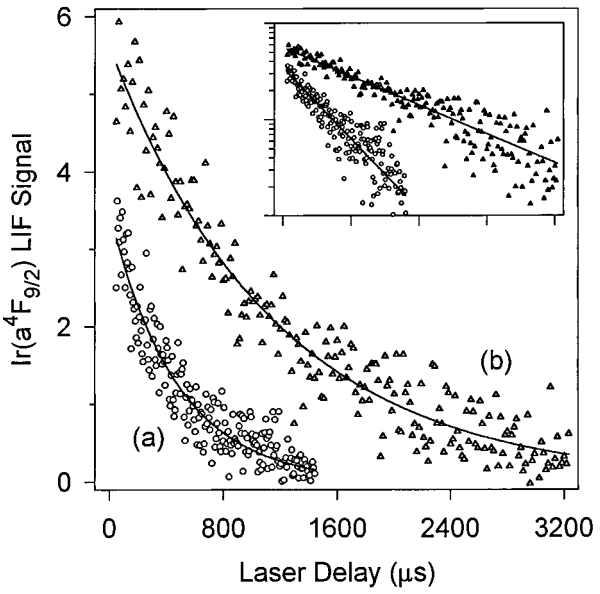

Figure 1. Typical Ir($a^4F_{9/2}$) decay curves with added CH_4. $T = 473$ K, $P_{total} = 50.0$ Torr, $P(SF_6) = 15$ Torr. (a) $P(CH_4) = 15.6$ Torr, $\tau = 450$ μs; (b) $P(CH_4) = 5.30$ Torr, $\tau = 1060$ μs. The solid lines through the data are exponential fits. The inset is a ln plot of the data.

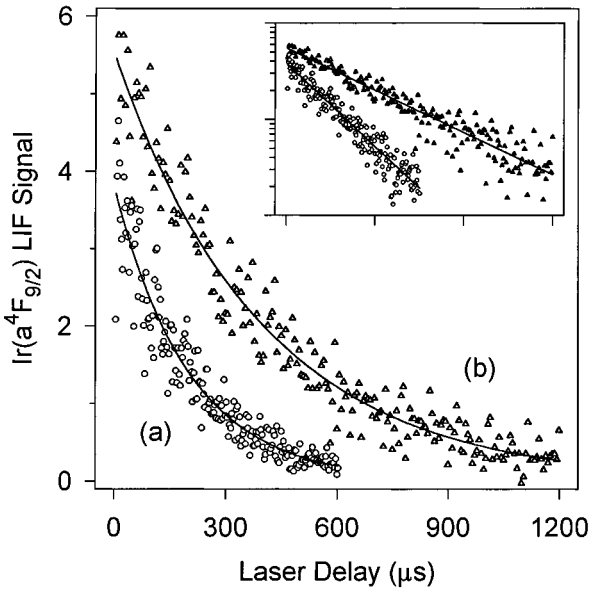

Figure 2. Typical Ir($a^4F_{9/2}$) decay curves with added O_2 or N_2O. $T = 296$ K. (a) $P(O_2) = 0.102$ Torr, $P_{total} = 10$ Torr, $P(CH_4) = 4.0$ Torr, $\tau = 200$ μs; (b) $P(N_2O) = 11.5$ Torr, $P_{total} = 200$ Torr, $P(CH_4) = 4.2$ Torr, $\tau = 383$ μs. The solid lines through the data are exponential fits. The inset is a ln plot of the data.

photodiode. LIF decay traces consisted of 200 points, each point averaged for four laser shots.

Materials. Dicarbonyl(acetylacetonato)iridium(I) (Strem, 99%), O_2 (MG Industries, 99.8%), N_2O (MG Industries, electronic grade, 99.999%), CH_4 (Linde, ultrahigh purity grade, 99.99%), SF_6 (Air Products, 99.9%), and N_2 (Potomac Airgas, Inc., 99.998%) were used as received.

Data Analysis and Results

The decay rates of the ground state ($a^4F_{9/2}$) of iridium as a function of reactant pressure were investigated as a function of temperature and total pressure. In the absence of a quencher gas, the decay profiles showed growth (i.e., nonexponential behavior) at the beginning of the decays. We attribute this behavior to the relaxation of electronically excited states to the ground state. Two polyatomic gases, CH_4 and SF_6, were found to efficiently relax the excited electronic states at room temperature without reacting with the ground state. Methane, however, could not be used at elevated temperatures due to chemical reaction. Methane appeared to be the better quencher at room temperature based on the appearance of the iridium temporal profiles in the absence of reactant. Thus, for the study of the O_2 and N_2O reactions at room temperature, approximately 4 Torr of methane was added as a quencher gas. Variations in the methane pressure from 4 to 19 Torr gave rate constants equal to within experimental uncertainty. Thus, methane pressures of 4 Torr or greater appear to sufficiently relax the excited states. Rate constants measured at elevated temperatures used SF_6 as the quencher gas.

Once the excited states have relaxed to the ground state, the loss of ground-state iridium is described by the first-order decay constant, k_1:

$$k_1 = 1/\tau = k_d + k_2[\text{oxid}] \qquad (1)$$

where τ is the first-order time constant for the removal of iridium under the given experimental conditions, k_d is the loss term due to diffusion out of the detection zone and reaction with the precursor and precursor fragments, and k_2 is the second-order rate constant. Typical decay profiles are shown in Figures 1 and 2. A time constant, τ, for each decay profile was determined using a linear least-squares procedure. Time constants were

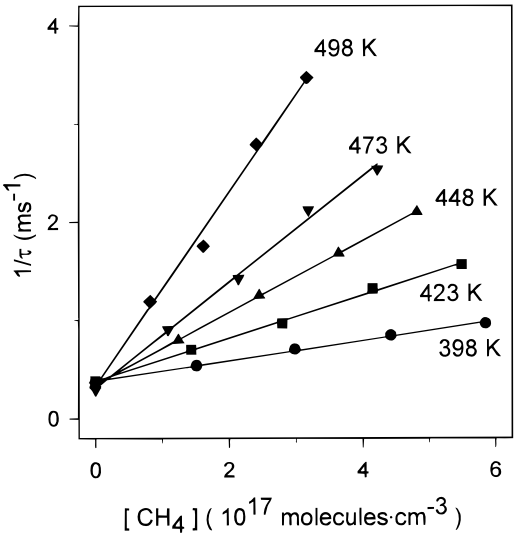

Figure 3. Typical plots for determining k_{2nd} for Ir($a^4F_{9/2}$) + CH_4 illustrating the large dependence of the bimolecular rate constants on temperature. The solid line for each set of data is a linear regression fit from which k_{2nd} is obtained.

determined by adjusting the range of the linear regression analysis; i.e., the range did not include the beginning of the decay when growth was present. Decays were typically analyzed after a delay of up to one reaction lifetime and included data for a length of two to three reaction lifetimes. Lifetimes of Ir($a^4F_{9/2}$) without oxidant were typically 2000 μs or greater, indicating diffusion out of the detection zone is inconsequential in these experiments.

The second-order rate constant is determined from a plot of $1/\tau$ vs reactant number density. Typical plots for obtaining second-order rate constants are presented in Figures 3 and 4; the slope yields the observed rate constant. The relative uncertainty (i.e., the reproducibility) of the second-order rate constants is estimated at ±20% based on repeated measurements of rate constants under identical temperature and total pressure conditions. The absolute uncertainties are conservatively estimated to be ±40% and are based on the sum of the statistical scatter in the data, uncertainty in the flowmeter and flow

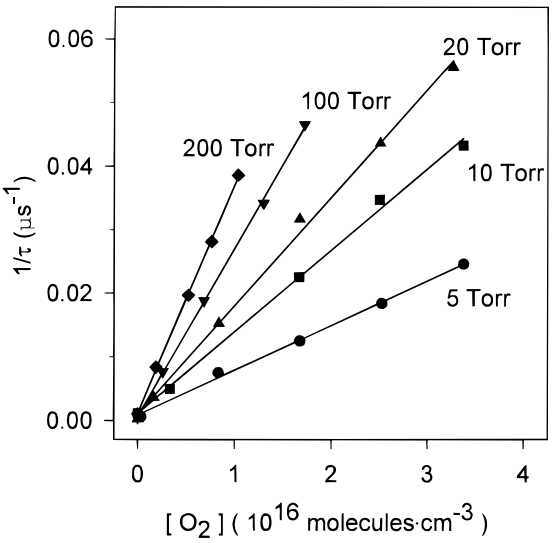

Figure 4. Typical plots for determining k_{2nd} for Ir($a^4F_{9/2}$) + O_2, indicating the dependence of the second-order rate constants on total pressure. The solid line for each set of data is a linear regression fit from which k_{2nd} is obtained.

TABLE 1: Second-Order Rate Constants (k_{2nd}, 10^{-15} cm^3 s^{-1}) for Ir($a^4F_{9/2}$) + CH_4 at 50 Torr

temp (K)	k_{2nd}	temp (K)	k_{2nd}
398	1.0	473	5.7
423	2.2	498	9.9
448	3.7		

controller readings (5%) and the total pressure reading (1%), uncertainties due to incomplete gas mixing, and uncertainties due to incomplete relaxation of the excited electronic states to the ground state.

Measured rate constants for the $a^4F_{9/2}$ state reacting with CH_4 at 50 Torr total pressure from 398 to 498 K are listed in Table 1. Rate constants could not be measured above 498 K due to thermal decomposition of the precursor. Below 398 K, the rate constants are too small to be measured reliably using our methods; i.e., under the experimental conditions employed in this study, the sensitivity (lower limit) of our apparatus is 1×10^{-15} cm^3 s^{-1}. The rate constants at 498 K were measured at 10, 20, and 50 Torr and are independent of total pressure within experimental uncertainty. An Arrhenius plot of the rate constants is shown in Figure 5. The rate constants are described by

$$k(T) = (7 \pm 5) \times 10^{-11} \exp(-37 \pm 3 \text{ kJ/mol}/RT) \quad (2)$$

where the uncertainties are $\pm 2\sigma$.

Measured rate constants for the $a^4F_{9/2}$ state reacting with O_2 and N_2O in nitrogen buffer at various pressures are listed in Tables 2 and 3. The rate constants are dependent on total pressure, indicating termolecular processes. The addition of methane as a quencher gas raises the possibility that the quencher gas may affect the rate constants due to the different efficiency of the stabilization of the adduct by each gas. However, rate constants measured with varying amounts of methane (from 4 to 19 Torr at $P_{tot} = 20$ Torr) gave rate constants equal to within experimental uncertainty. Thus, CH_4 and N_2 appear to stabilize the adduct with approximately equal efficiency. Rate constants for these reactions were essentially temperature invariant up to 498 K, indicating, at most, small barriers in these processes. The variation with total pressure of the second-order rate constants at room temperature in N_2 buffer are shown in Figure 6. The solid lines through the data in Figure 6 are weighted fits to the simplified Lindemann−

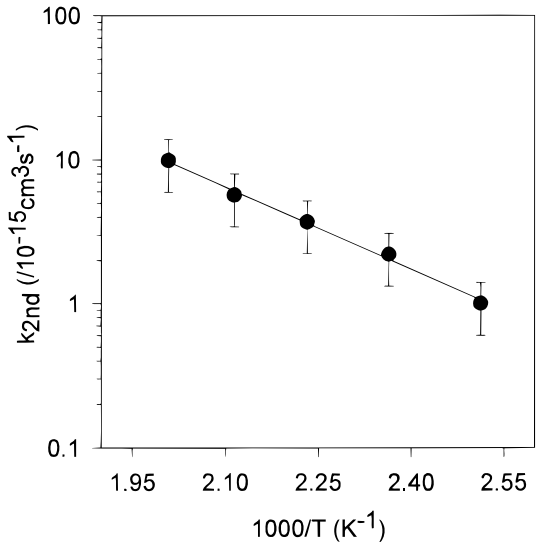

Figure 5. Arrhenius plot for the collisional disappearance of Ir($a^4F_{9/2}$) with CH_4. Error bars represent ±40% uncertainty.

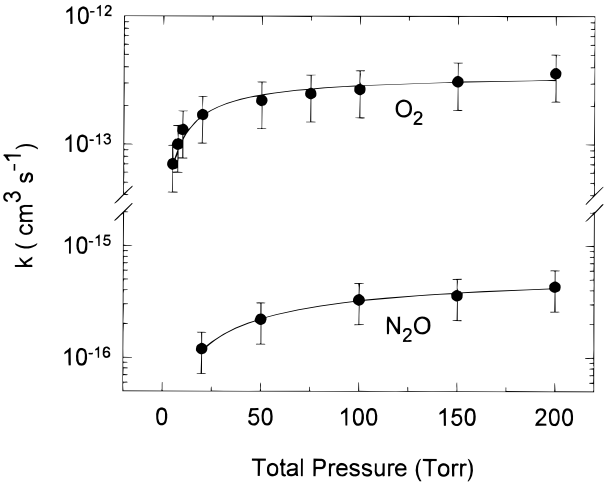

Figure 6. Pressure dependence of the reaction of Ir($a^4F_{9/2}$) with O_2 and N_2O in N_2 buffer at room temperature. Error bars represent ±40% uncertainty. The solid lines are fits to eq 3.

TABLE 2: Second-Order Rate Constants (k_{2nd}, 10^{-12} cm^3 s^{-1}) for Ir($a^4F_{9/2}$) + O_2 in N_2 Buffer at 296 K

total press. (Torr)	k_{2nd}	total press. (Torr)	k_{2nd}
5	0.70	75	2.5
7.5	1.0	100	2.7
10	1.3	150	3.1
20	1.7	200	3.6
50	2.2		

TABLE 3: Second-Order Rate Constants (k_{2nd}, 10^{-15} cm^3 s^{-1}) for Ir($a^4F_{9/2}$) + N_2O in N_2 Buffer at 296 K

total press. (Torr)	k_{2nd}	total press. (Torr)	k_{2nd}
20	1.2	150	3.6
50	2.2	200	4.3
100	3.3		

Hinshelwood expression[32]

$$k = \frac{k_0[\text{M}]}{1 + k_0[\text{M}]/k_\infty} \quad (3)$$

where k_0 is the limiting low-pressure third-order rate constant, k_∞ is the limiting high-pressure second-order rate constant, and [M] is the buffer gas number density. The values for k_0 and k_∞ for the reaction of O_2 in N_2 buffer at room temperature are $(4.8 \pm 1.6) \times 10^{-30}$ cm^6 s^{-1} and $(3.6 \pm 0.4) \times 10^{-12}$ cm^3 s^{-1},

respectively. The values for k_0 and k_∞ for the reaction of N_2O in N_2 buffer at room temperature are $(2.2 \pm 0.5) \times 10^{-33}$ cm^6 s^{-1} and $(5.9 \pm 0.8) \times 10^{-15}$ cm^3 s^{-1}, respectively. The listed uncertainties are $\pm 2\sigma$.

Discussion

Ir + CH_4. The two most plausible reaction pathways for the reaction of iridium with methane are the termolecular insertion channel to produce H−Ir−CH_3 and the bimolecular H_2 elimination reaction to produce Ir═CH_2. Assuming the reaction has not reached its high-pressure limit at 10 Torr, the experimental results reported here are consistent with a bimolecular mechanism. Thus, the most likely reaction channel is the H_2 elimination reaction.

Of the three reactions reported here, extensive calculations have only been performed for the reaction of iridium with methane. A condensation of the primary findings reported by Carroll et al follows.[11] PCI-80 calculations for iridium reacting with methane indicate the $6s^25d^7$ electronic state is an important factor in the dynamics of this reaction. The presence of the two s electrons makes this state highly repulsive toward methane, and no energy minimum is found along the potential energy surface for this state. The attractive surface that correlates with the strongly bound H−Ir−CH_3 insertion product arises from the low-spin $a^2P_{3/2}$ asymptote which lies 126 kJ/mol above the ground-state reactants. The quartet and doublet molecular iridium adducts crossing occurs at an Ir−C distance of 2.2 Å and is 75 kJ/mol above the ground-state asymptote. Once the reactants reach the low-spin surface, there is probably no barrier to formation of the C−H insertion product. The C−H insertion product is calculated to be 52.7 kJ/mol bound relative to the ground-state reactants. Elimination of H_2 from the insertion product is calculated to be 66.5 kJ/mol higher in energy than the reactants. Thus, calculations predict a very slow reaction at room temperature which was consistent with the observance of no reaction reported previously.[11]

Since the crossing for the ground-state surface at 75 kJ/mol is higher than the endoergicity of the H_2 elimination reaction, reactants that overcome this barrier have the required energy to go on to eliminate H_2. Thus, the calculations indicate once the energy barrier has been surmounted along the ground-state surface, reaction should proceed to H_2 elimination. The calculations, however, predict a barrier approximately double the value determined here experimentally. Thus, qualitatively the calculations are consistent with experiment in predicting the H_2 elimination mechanism while the quantitative discrepancy for the size of the barrier is larger than can be accounted for by experimental error.

The activation energy reported here for the reaction of iridium with methane yields a lower limit to the Ir═C bond energy in the $IrCH_2$ product. The formation of methylene and diatomic hydrogen from methane in the absence of iridium is calculated to have an endoergicity of 457 kJ/mol.[33] Since the endoergicity of the reaction of iridium with methane can be no larger than its activation energy (37 kJ/mol), the lower limit to the Ir═C bond energy is thus determined to be 420 kJ/mol. The PCI-80 calculation of the Ir═C bond energy (378 kJ/mol) is 10% smaller than our experimentally determined lower limit.[11]

Ir + O_2. Results for the reaction of iridium with O_2 indicate a termolecular insertion reaction mechanism.

$$\mathrm{Ir}(a^4F_{9/2}) + O_2 \xrightarrow{[N_2]} \mathrm{IrO_2} \qquad (4)$$

IrO_2 has been observed previously from the reaction of laser-vaporized iridium metal with O_2.[34] IrO_2 was found to be linear ($D_{\infty h}$) with a $^2\Sigma$ electronic ground state. The bimolecular abstraction mechanism to produce IrO is endothermic by 87 kJ/mol;[33,35] thus, the thermodynamic barrier prohibits this pathway at the temperatures studied here.

The value of the limiting low-pressure third-order rate constant is large compared to other termolecular reactions with O_2 involving s^2d^{n-2} transition metals. A comparison of the low-pressure third-order rate constant with that of another group 9 atom, $4s^23d^7$ $a^4F_{9/2}$ Co, indicates the rate constant for iridium is approximately 400 times greater than the rate constant for cobalt.[27] In fact, the rate constants for iridium are similar in magnitude to TMs with s^1d^{n-1} configurations. Previous studies of the 3d transition-metal association reactions with O_2 indicate that TMs with ground-state or low-lying s^1d^{n-1} configurations are reactive whereas TMs with s^2d^{n-2} ground-state configurations are unreactive.[27] This behavior has been explained in terms of simple molecular orbital concepts. In the approach of the TM to O_2, the nature of the potential in the region of the onset of orbital overlap will be determined by the interaction between the s-orbital of the TM atom (which has a larger spatial extent than the d-orbitals) and the in-plane π*-antibonding orbital of O_2. For a TM atom with an s^1 configuration, an electron pair bond may be formed from the overlap of these orbitals, as in a radical−radical recombination process. In the case of an s^2 configuration, one of the s-electrons occupies the antibonding molecular orbital between the TM atom and O_2, which destabilizes the complex and leads to a less attractive or a repulsive potential.[27] Iridium's relatively large reactivity may be related to the low-lying $6s^15d^8$ $b^4F_{9/2}$ state only 2835 cm^{-1} above the ground state.[36] It is conceivable that the surface hopping from the ground state to the s^1d^8 excited surface is reasonably efficient, resulting in the unusually fast reaction compared to other TMs with s^2 configurations.

The value of k_∞ for this reaction is about 1−2 orders of magnitude smaller than values of k_∞ for TMs with s^1d^{n-1} configurations reacting with O_2.[23] One factor that causes a depression of the value of k_∞ for this reaction is the much smaller electronic degeneracy of the activated complex compared to the degeneracies of the reactants. According to transition-state theory,[37] k_∞ for a recombination reaction is proportional to the ratio of the partition functions of the activated complex to the product of the partition functions of the reactants; i.e., $k_\infty \propto Q(IrO_2^\dagger)/Q(Ir)Q(O_2)$. Assuming the electronic state of the activated complex is the $^2\Sigma$ state observed for the IrO_2 insertion product,[34] the electronic contribution to the partition function ratio is approximately 1/15 since $Q_{elect}(IrO_2^\dagger) \approx 2$, $Q_{elect}(Ir) \approx 10$, and $Q_{elect}(O_2) \approx 3$. Thus, the electronic contribution represents a depression of about an order of magnitude in k_∞. The small value of k_∞ may also be due to the less than unity probability of the s^2d^{n-2} to s^1d^{n-1} surface hopping process. Confirmation of the importance of the excited-state surface's contribution to this reaction awaits accurate calculations.

Ir + N_2O. Results for the reaction of iridium with N_2O indicate a very weakly bound adduct:

$$\mathrm{Ir}(a^4F_{9/2}) + N_2O \xrightarrow{[N_2]} \mathrm{IrON_2} \qquad (5)$$

where it is not known to which atom(s) the iridium is bound or the geometry of the adduct. While measurable, the rate constants are extremely small (near the lower limit of the apparatus), indicating a very inefficient process. No other termolecular processes involving a TM with N_2O have been reported previously, although recent experiments in our laboratory indicate the reactions of platinum and nickel with N_2O are pressure-dependent. For both platinum and nickel, at a given pressure, the rate constants of these metals are approximately 2 orders of magnitude larger than those of iridium, while a

bimolecular abstraction channel component is also indicated.[38,39] The abstraction component is indicated for these metals by a nonzero intercept in the pressure dependence of the rate constants and a positive temperature dependence of the rate constants. There are no such indications of a bimolecular component for the reaction of N_2O with iridium in the experiments reported here.

Abstraction reactions of all TM atoms with N_2O are exothermic due to the formation of the stable N_2 and metal oxide molecules. Despite this exothermicity, metal atom reactions with N_2O have been observed to have significant energy barriers. These barriers have been attributed to the requirement of a nonadiabatic transition along the reaction pathway.[40] For iridium reacting with N_2O to produce IrO, the abstraction reaction is exothermic by 244 kJ/mol.[33,35] Experimentally, we were unable to detect a bimolecular component for this reaction up to a temperature of 498 K. Assuming a maximum value of 1×10^{-15} cm^3 s^{-1} for the rate constant for the abstraction channel at 498 K and assuming a preexponential factor of 5×10^{-11} cm^3 s^{-1}, an estimate of the minimum activation energy for this reaction is calculated to be approximately 45 kJ/mol. This minimum barrier is similar to the experimentally measured activation energy for the abstraction reaction of $4s^23d^7$ $a^4F_{9/2}$ Co with N_2O ($E_a = 49$ kJ/mol).[39]

Recently, Fontijn and co-workers have advanced a resonance interaction model[41−44] to predict barriers to reaction and rate constants for metal atoms reacting with N_2O. In this model, the activation barriers are calculated by taking into account the ionization potential and sp promotion energy of the metal, the electron affinity of N_2O, and the bond energy of the metal oxide product. The resonance interaction model predicts the energy barrier for the reaction of iridium with N_2O to be 41 kJ/mol,[41] a value slightly smaller than our lower estimate.

Summary

We have measured the rate constants as a function of temperature and pressure for the reaction of ground-state iridium ($a^4F_{9/2}$) with CH_4, O_2, and N_2O. The reaction of iridium with CH_4 is consistent with a bimolecular H_2 elimination reaction. The reaction is slow with an activation energy of 37 kJ/mol. The reaction of ground-state iridium with O_2 and N_2O involves termolecular processes. For O_2, the reaction is rapid compared to other termolecular reactions involving s^2d^{n-2} transition metals. The rapidity of the reaction is attributed to a surface crossing with the low-lying $6s^15d^8$ $b^4F_{9/2}$ electronic state. For N_2O, the termolecular reaction is very inefficient. There is no indication of the abstraction reaction channel up to a temperature of 498 K, indicating an activation energy of at least 45 kJ/mol.

Acknowledgment. This research was supported by a Cottrell College Science Award of Research Corporation. Acknowledgment is made to the donors of the Petroleum Research Fund, administered by the American Chemical Society, for partial support of this research.

References and Notes

(1) Eller, K.; Schwarz, H. *Chem. Rev. (Washington, D.C.)* **1991**, *91*, 1121.
(2) Weisshaar, J. C. *Acc. Chem. Res* **1993**, *26*, 213.
(3) Elkind, J. L.; Armentrout, P. B. *J. Phys. Chem.* **1987**, *91*, 2037.
(4) Armentrout, P. B. In *Gas-Phase Inorganic Chemistry*; Russell, D. H., Ed.; Plenum: New York, 1989.
(5) Armentrout, P. B. *Annu. Rev. Phys. Chem.* **1990**, *41*, 313.
(6) Ritter, D.; Weisshaar, J. C. *J. Am. Chem. Soc.* **1990**, *112*, 6425.
(7) Ritter, D.; Carroll, J. J.; Weisshaar, J. C. *J. Phys. Chem.* **1992**, *96*, 10636.
(8) Carroll, J. J.; Weisshaar, J. C. *J. Am. Chem. Soc.* **1993**, *115*, 800.
(9) Carroll, J. J.; Haug, K. L.; Weisshaar, J. C. *J. Am. Chem. Soc.* **1993**, *115*, 6962.
(10) Carroll, J. J.; Haug, K. L.; Weisshaar, J. C.; Blomberg, M. R. A.; Siegbahn, P. E. M.; Svensson, M. *J. Phys. Chem.* **1995**, *99*, 13955.
(11) Carroll, J. J.; Weisshaar, J. C.; Siegbahn, P. E. M.; Wittborn, C. A. M.; Blomberg, M. R. A. *J. Phys. Chem.* **1995**, *99*, 14388.
(12) Carroll, J. J.; Weisshaar, J. C. *J. Phys. Chem.* **1996**, *100*, 12355.
(13) Wen, Y.; Yethiraj, A.; Weisshaar, J. C. *J. Chem. Phys.* **1997**, *106*, 5509.
(14) Blitz, M. A.; Mitchell, S. A.; Hackett, P. A. *J. Phys. Chem.* **1991**, *95*, 8719.
(15) Brown, C. E.; Mitchell, S. A.; Hackett, P. A. *Chem. Phys. Lett.* **1992**, *191*, 175.
(16) Lian, L.; Mitchell, S. A.; Rayner, D. M. *J. Phys. Chem.* **1994**, *98*, 11637.
(17) Parnis, J. M.; Lafleur, R. D.; Rayner, D. M. *J. Phys. Chem.* **1995**, *99*, 673.
(18) Senba, K.; Matsui, R.; Honma, K. *J. Phys. Chem.* **1995**, *99*, 13992.
(19) Campbell, M. L. *J. Am. Chem. Soc.* **1997**, *119*, 5984.
(20) Campbell, M. L.; McClean, R. E. *J. Chem. Soc., Faraday Trans.* **1995**, *91*, 3787.
(21) McClean, R. E.; Campbell, M. L.; Goodwin, R. H. *J. Phys. Chem.* **1996**, *100*, 7502.
(22) Harter, J. S. S.; Campbell, M. L.; McClean, R. E. *Int. J. Chem. Kinet.* **1997**, 29, 367.
(23) Campbell, M. L. *J. Chem. Soc., Faraday Trans.* **1996**, *92*, 4377.
(24) McClean, R. E.; Campbell, M. L.; Kölsch, E. J. *J. Phys. Chem. A* **1997**, *101*, 3348.
(25) Campbell, M. L.; Hooper, K. L. *J. Chem. Soc., Faraday Trans.* **1997**, *93*, 2139.
(26) Campbell, M. L.; Hooper, K. L.; Kölsch, E. J. *Chem. Phys. Lett.* **1997**, *274*, 7.
(27) Brown, C. E.; Mitchell, S. A.; Hackett, P. A. *J. Phys. Chem.* **1991**, *95*, 1062.
(28) Matsui, R.; Senba, K.; Honma, K. *J. Phys. Chem. A* **1997**, *101*, 179.
(29) Fontijn, A.; Blue, A. S.; Narayan, A. S.; Bajaj, P. N. *Combust. Sci. Technol.* **1994**, *101*, 59.
(30) Meggers, W. F.; Corliss, C. H.; Scribner, B. F. *Tables of Spectral-Line Intensities, Part I Arranged by Elements*; NBS Monograph 145; U.S. Government Printing Office: Washington, DC, 1975.
(31) Gough, D. S.; Hannaford, P.; Lowe, R. M. *J. Phys. B: At. Mol. Phys.* **1983**, *16*, 785.
(32) Robinson, P. J.; Holbrook, K. A. *Unimolecular Reactions*; Wiley-Interscience: New York, 1972.
(33) Wagman, D. D.; Evans, W. H.; Parker, V. B.; Schumm, R. H.; Halow, I.; Bailey, S. M.; Churney, K. L.; Nuttall, R. L. *J. Phys. Chem. Ref. Data* **1982**, *11* (Suppl. 2).
(34) Van Zee, R. J.; Hamrick, Y. M.; Li, S.; Weltner, Jr., W. *J. Phys. Chem.* **1992**, *96*, 7247.
(35) Pedley, J. B.; Marshall, E. M. *J. Phys. Chem. Ref. Data* **1983**, *12*, 967.
(36) Moore, C. E. *NBS Circular 467*; U.S. Department of Commerce: Washington, DC, 1971; Vol. III.
(37) Gilbert, R. G.; Smith, S. C. *Theory of Unimolecular and Recombination Reactions*; Blackwell Scientific: Oxford, 1990; p 49.
(38) Campbell, M. L. *J. Chem. Soc., Faraday Trans.*, in press.
(39) (a) Kölsch, E. J. *Trident Scholar Project Report No. 249*; USNA Printing Office: Annapolis, MD, 1997. (b) Campbell, M. L.; Kölsch, E. J.; Hooper, K. L., manuscript in preparation.
(40) Jonah, C. D.; Zare, R. N.; Ottinger, C. J. *J. Chem. Phys.* **1972**, *56*, 263.
(41) Futerko, P. M.; Fontijn, A. *J. Chem. Phys.* **1991**, *95*, 8065.
(42) Futerko, P. M.; Fontijn, A. *J. Chem. Phys.* **1992**, *97*, 3861.
(43) Futerko, P. M.; Fontijn, A. *J. Chem. Phys.* **1993**, *98*, 7004.
(44) Belyung, D. P.; Futerko, P. M.; Fontijn, A. *J. Chem. Phys.* **1995**, *102*, 155.